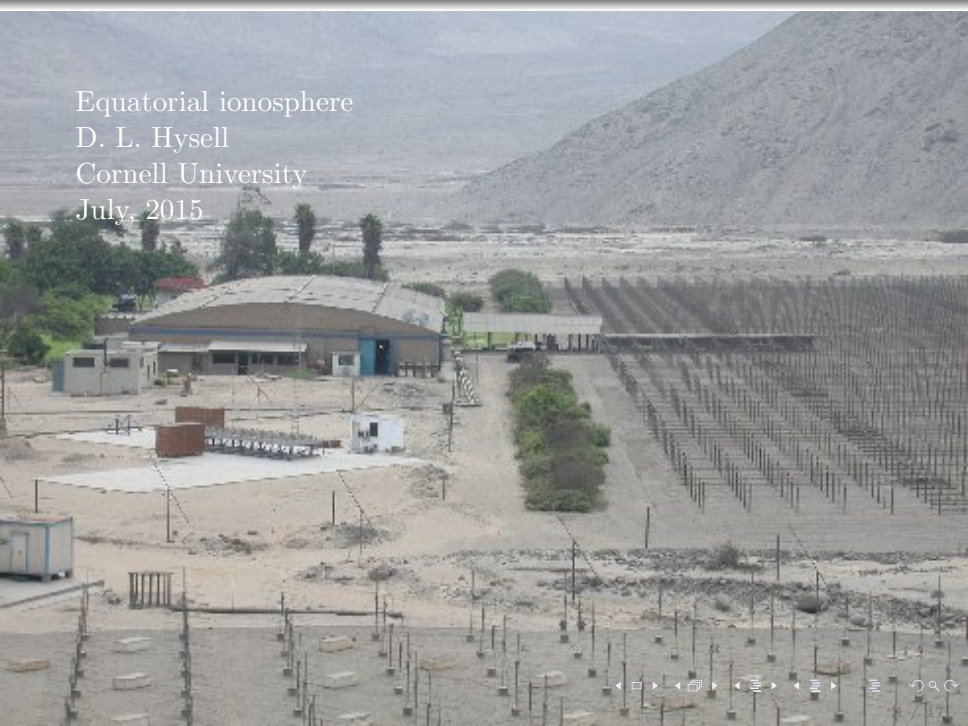


Equatorial ionosphere

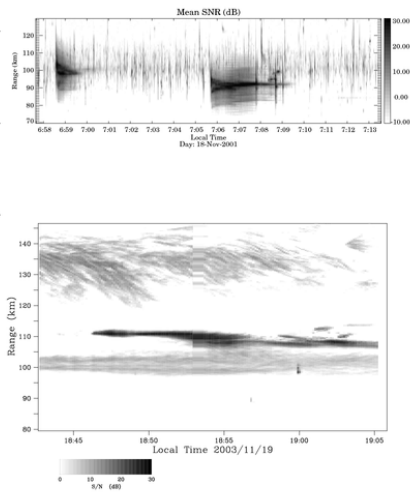
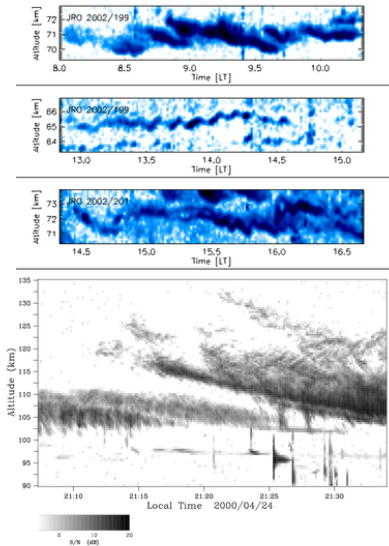
D. L. Hysell

Cornell University

July, 2015

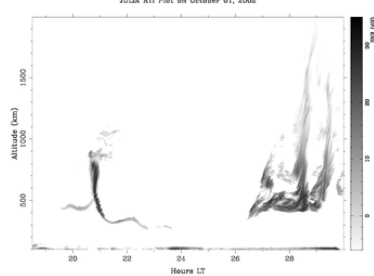
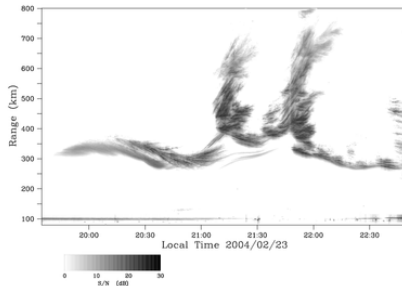
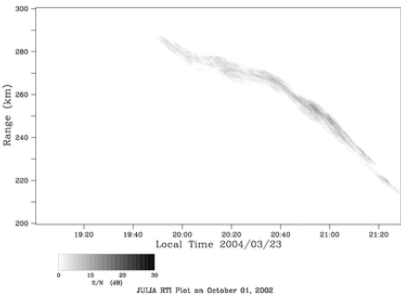
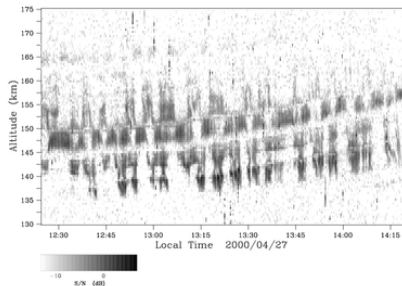


equatorial phenomena



movie

more examples



- survey of unique equatorial phenomena
- the geomagnetic field
- ionospheric structure
- plasma density, temperature, composition
- plasma drifts, dynamics; dynamo theory
- equatorial E region, electrojet
- neutral winds
- equatorial spread F

dipole magnetic field

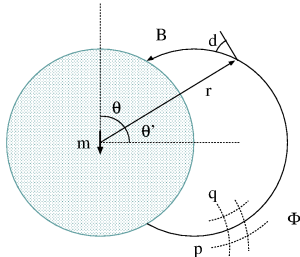
$$\phi_m = -\frac{\mathbf{m} \cdot \mathbf{r}}{r^3} = -\frac{\cos \theta}{r^2}$$

$$\mathbf{B} = -\nabla \phi_m = -\frac{2m \cos \theta}{r^3} \hat{r} - \frac{m \sin \theta}{r^3} \hat{\theta} = -\frac{3\hat{r}(\mathbf{m} \cdot \hat{r}) - \mathbf{m}}{r^3}$$

$$B = \frac{m}{r^3} (1 + 3 \cos^2 \theta)^{1/2}$$

$$\tan d = \frac{B_r}{B_\theta} = 2 \tan \theta'$$

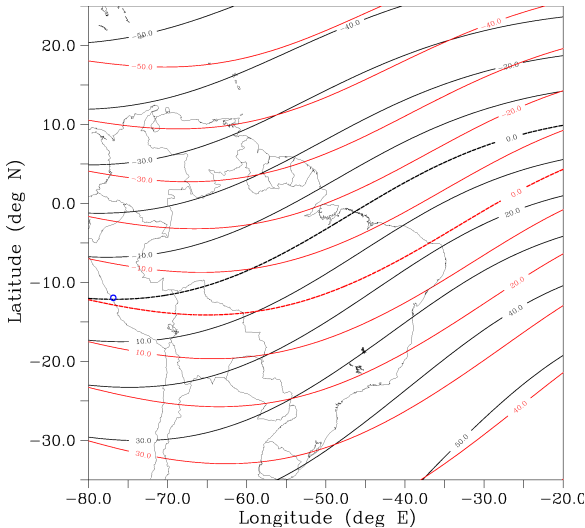
$$r = LR_e \sin^2 \theta \quad (p = r / \sin^2 \theta, q = \cos \theta / r^2, \Phi)$$



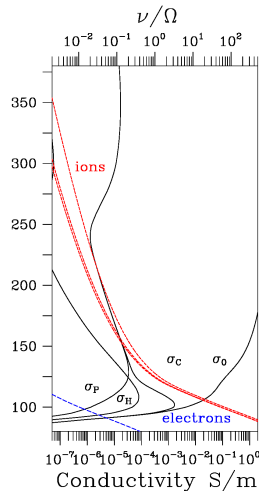
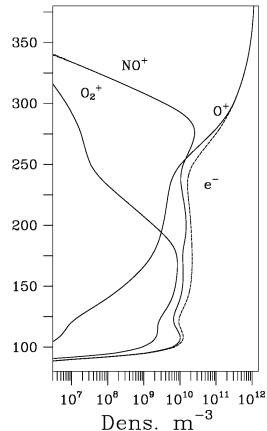
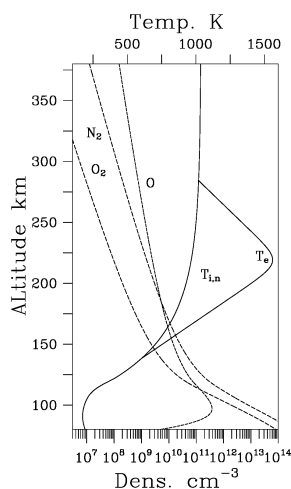
$$h_p = \sin^3 \theta / \delta, h_q = r^3 / \delta, h_\Phi = r \sin \theta$$

$$\delta = \sqrt{1 + 3 \cos^2 \theta}$$

non-dipole contribution



ionospheric structure (model)



high altitude ISR

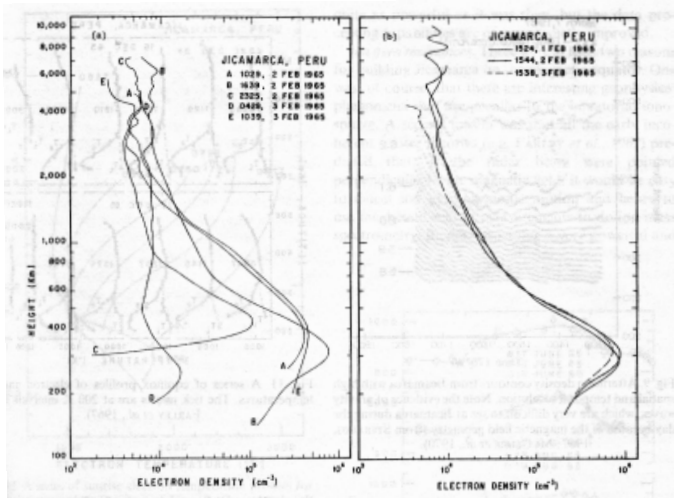
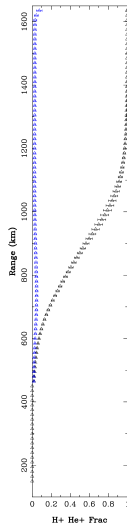
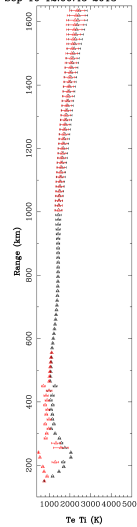
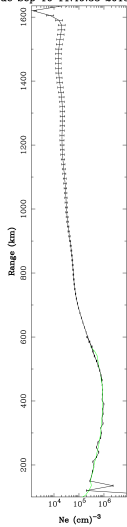
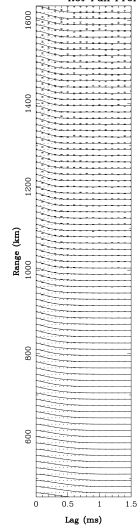
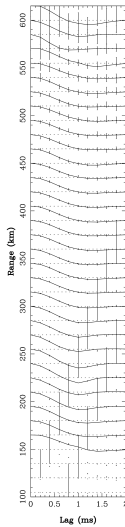


Fig. 8. Examples of the density profiles used for Fig. 6. Note the very small early morning value of N_{\max} in (a), and the consistency of the three afternoon profiles in (b) (from FARLEY, 1966a).

After D. T. Farley, *J. Atmos. Sol. Terr. Phys.*, 53, 665–675, 1991

profiles: 12 LT



temperature and composition

- At low altitudes, composition controlled by local photochemistry, temperature controlled by local heating and cooling.
- At higher altitudes, material and heat transport (diffusion, thermal diffusion) become important. Heat budget in topside also affected by energetic electron transport.
- Main topside light-ion reactions are $H^+ - O^+$ charge exchange for hydrogen ions and photoionization and charge exchange with molecular species for helium ions.

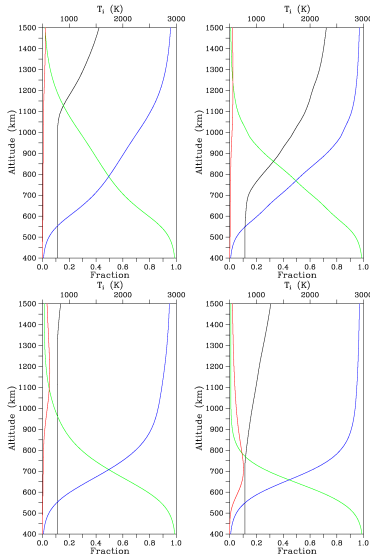
diffusive equilibrium (late afternoon)

$$0 = -K \nabla(n_j T)/n_j + eE - m_j g$$
$$0 = -K \nabla(n_e T)/n_e - eE$$

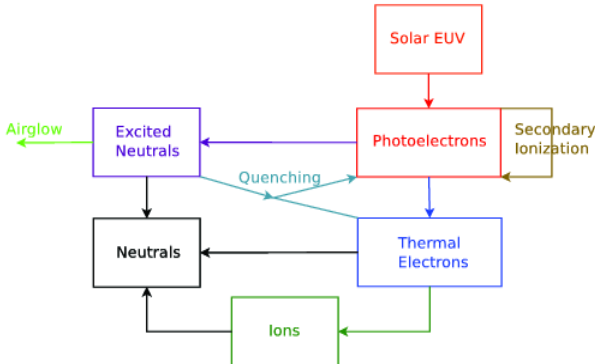
$$n_e = \sum_j n_j, \quad T_j = T_e = T$$

$$\frac{n_j(z)}{n_e(z)} = \frac{n_{oj} e^{-\int_{\odot}^z dz/H_j}}{\sum_i n_{oi} e^{-\int_{\odot}^z dz/H_i}}$$

$$H_j \equiv \frac{KT(z)}{m_j g(z)}$$



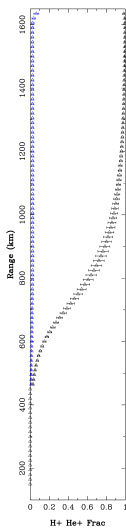
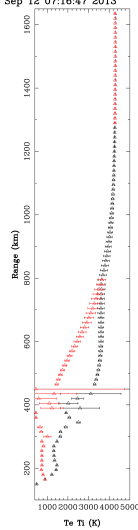
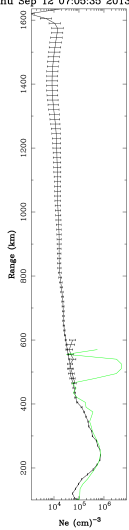
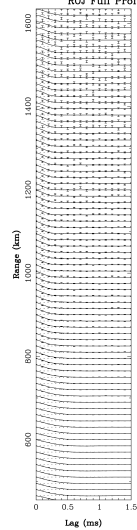
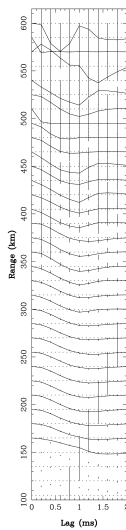
Equatorial ionosphere seldom in diffusive equilibrium!



from Varney, Cornell Univ., 2012

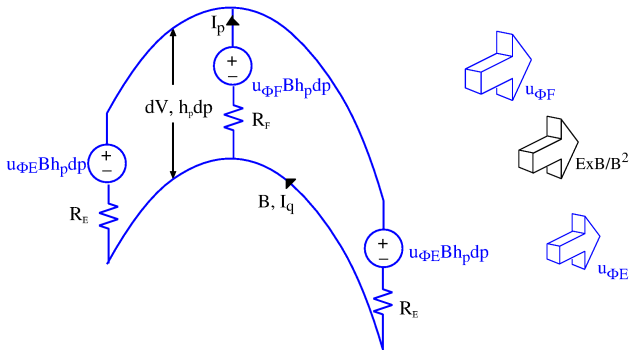
Photoelectrons degraded by pitch-angle scattering, elastic, and inelastic collisions as they propagate along B , preserve the 1st adiabatic invariant, undergo trapping, and ultimately return to the thermal electron population.

profiles: 07 LT



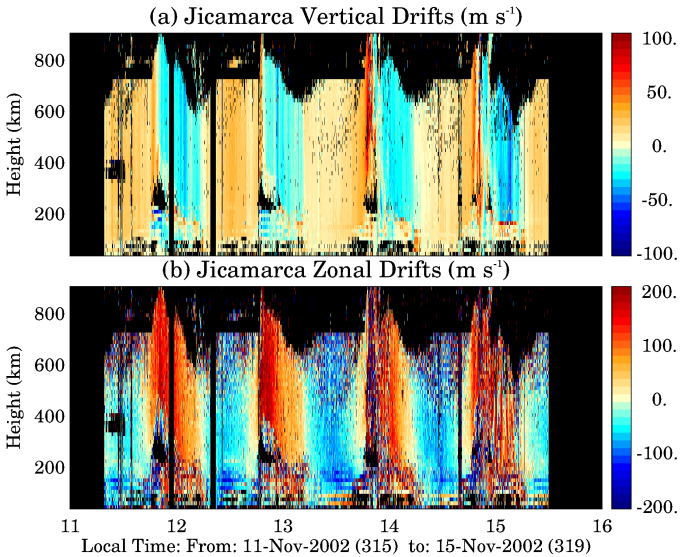
electrodynamics and dynamo theory: circuit analogy

- quasineutrality ($\nabla \cdot \mathbf{J} = 0$) and Faraday's law for electrostatics together with high direct conductivity imply Kirchhoff's laws for circuits

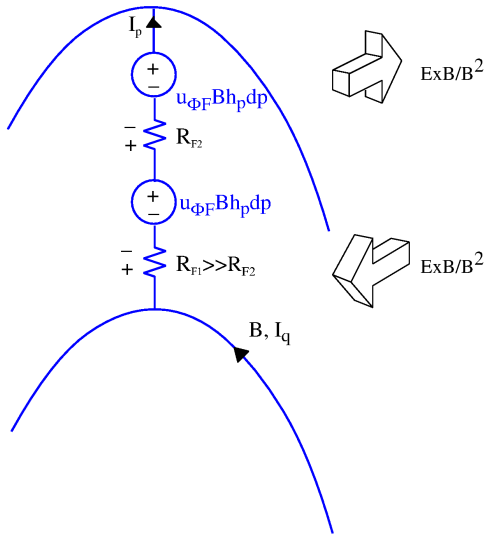


$$dV = \frac{u_{\Phi F} B h_p dp / R_F + u_{\Phi E} B h_p dp / R_E}{1/R_F + 1/R_E}$$

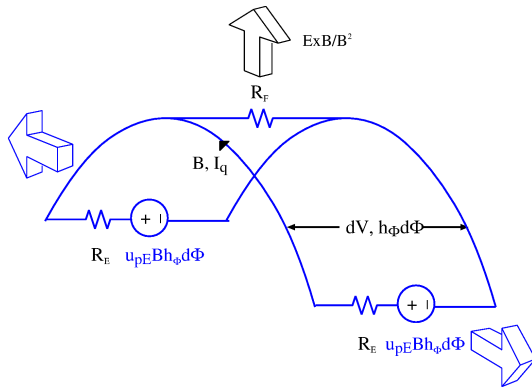
zonal drifts, super-rotation



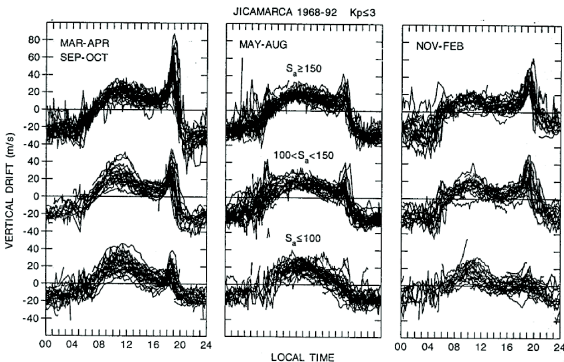
shear flow



vertical drifts (daytime)

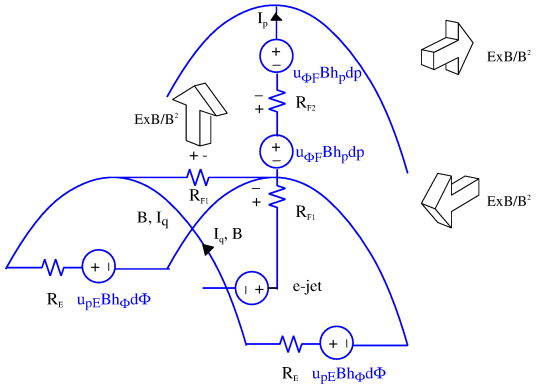


prereversal enhancement

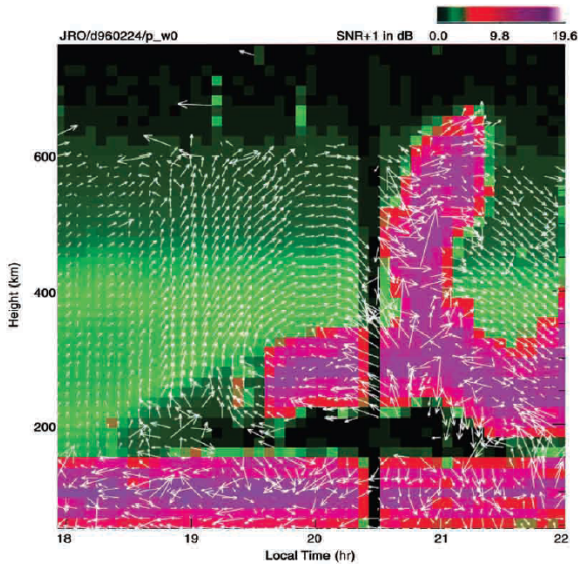


Scherliess and Fejer, *J. Geophys. Res.*, 104, 682, 1999

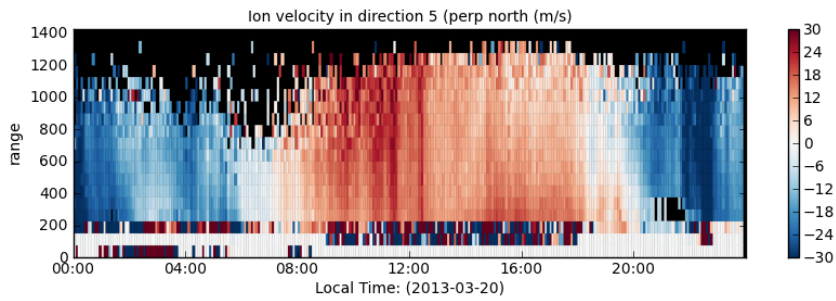
prereversal enhancement



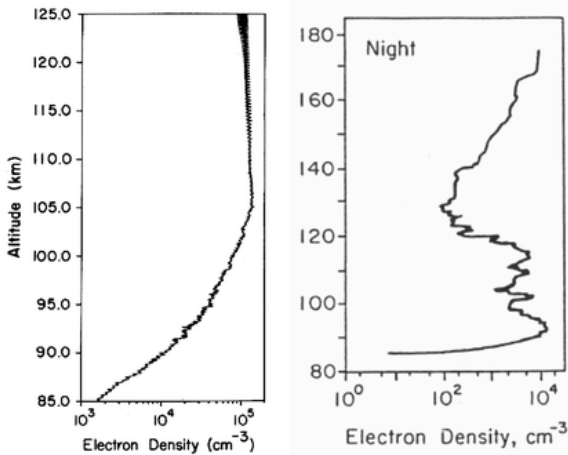
vorticity



topside drifts

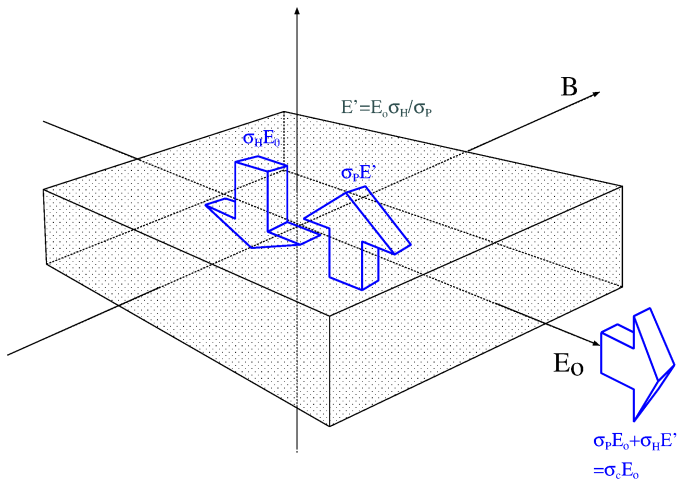


E layer



From Pfaff, *J. Atmos. Terr. Phys.*, 53, 709, 1991 and Prakash et al., *Indian J. Radio Space Phys.*, 72, 1, 1972.

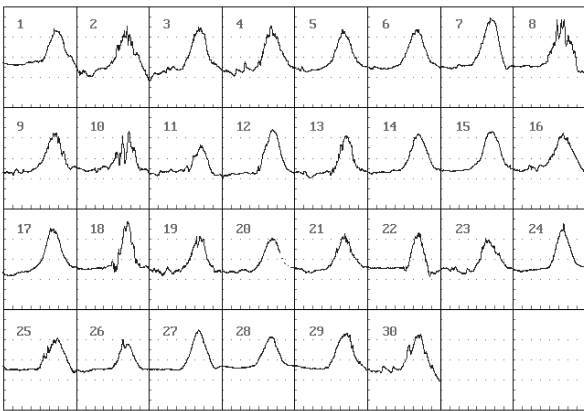
slab electrojet current model (daytime)



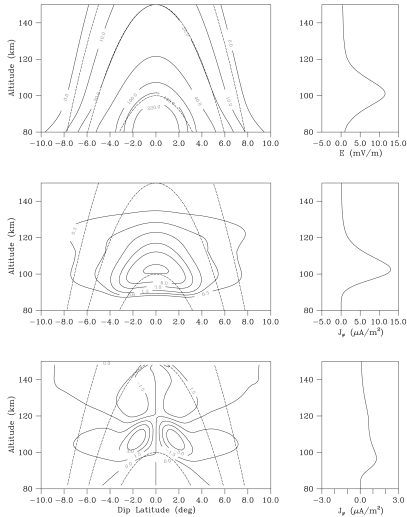
Jicamarca magnetometer

Estacion : Jicamarca - Peru
Fecha : JUNIO 2002

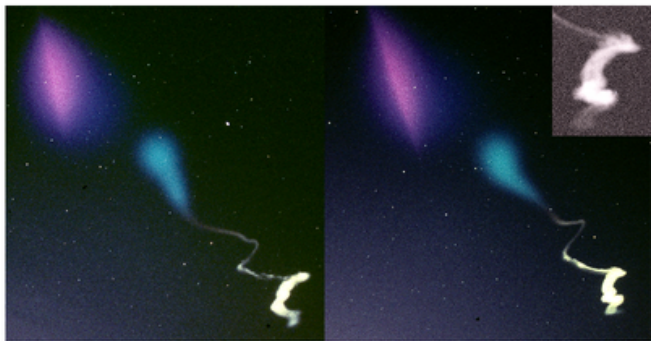
Comp. : H
Escala : 40 nT/Div



numerical model: $\nabla \cdot \mathbf{J} = 0$

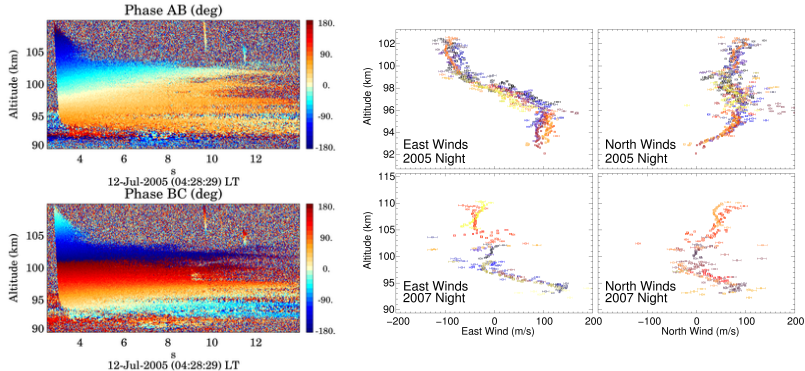


mlt winds



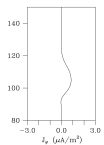
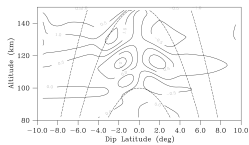
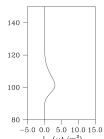
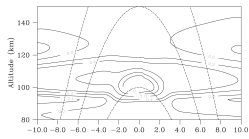
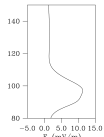
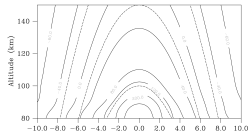
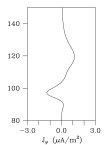
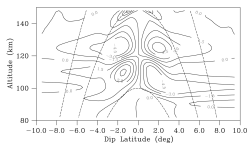
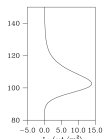
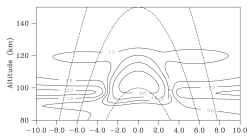
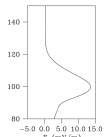
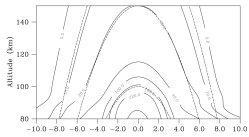
Larsen, M. F., *J. Geophys. Res.*, 107, 10.1029/2001JA000218, 2002.

meteor trail winds

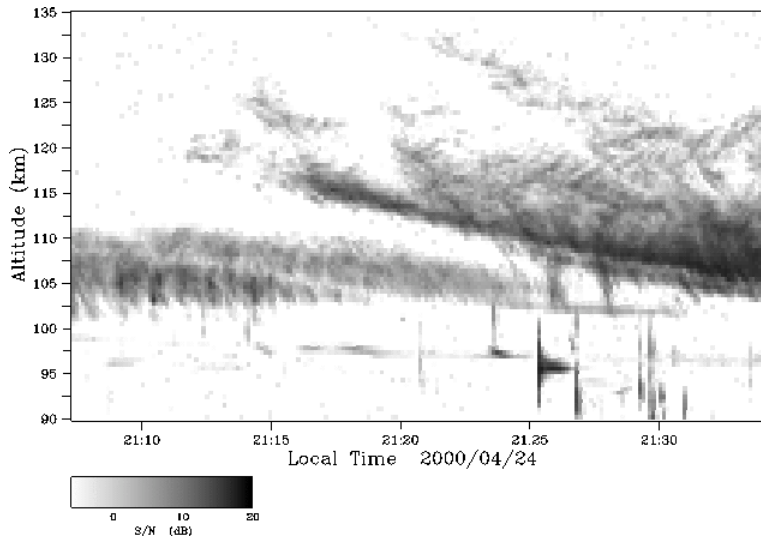


Oppenheim, M. M., et al., *Geophys. Res. Lett.*, 36, L09817, 2009

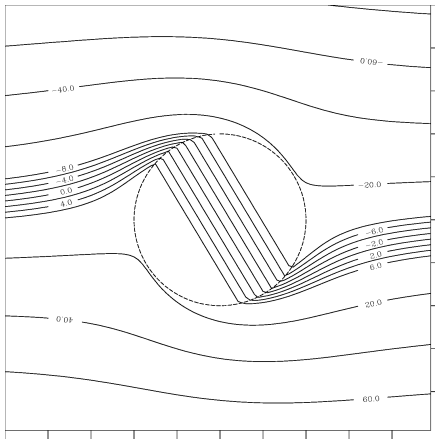
with TIME-GCM winds (noon, twilight)



electrojet plasma waves

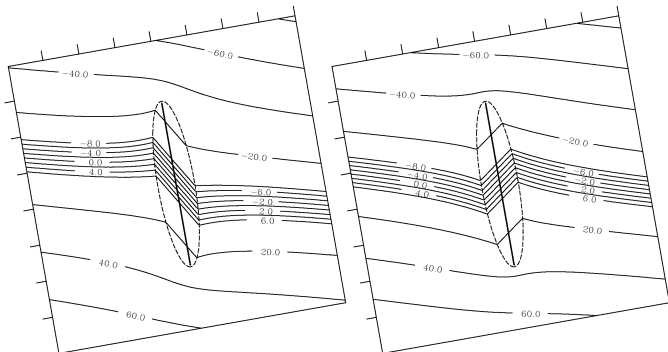


heuristic description of FBGD instability (daytime)



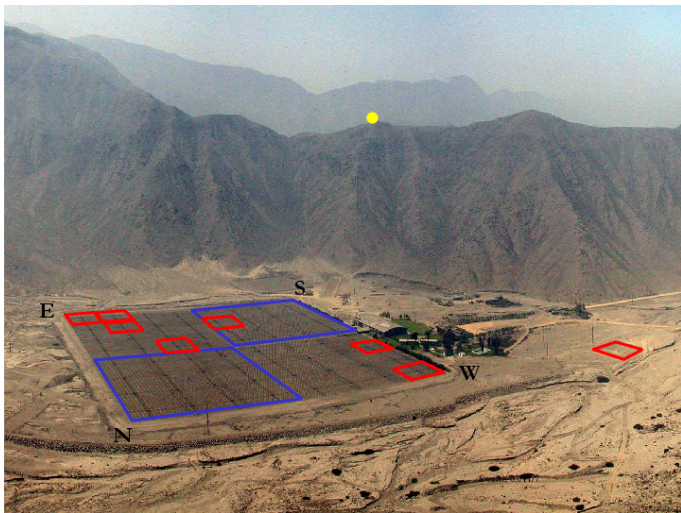
Solution of $\nabla \cdot \mathbf{J} = 0$ (equipotentials) for two-dimensional depletion interrupting electrojet current.

heuristic description of instability (daytime)



depletion — enhancement

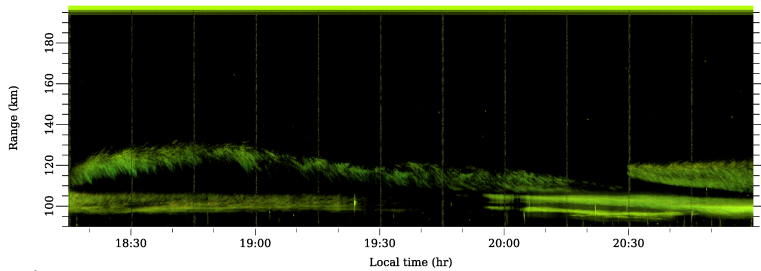
radar imagery



daytime nighttime

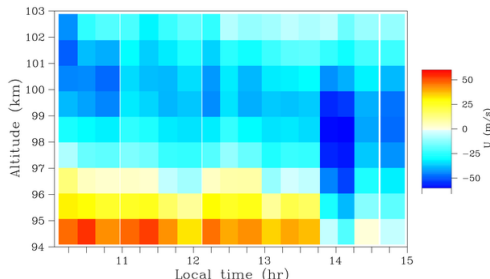
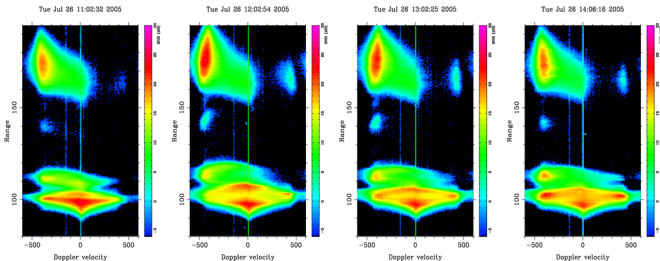
layered strata

Mon Sep 5 18:05:59 2011

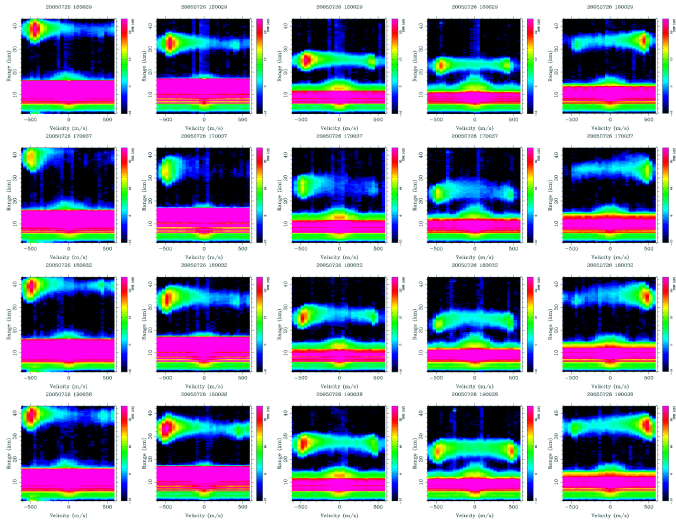


movie

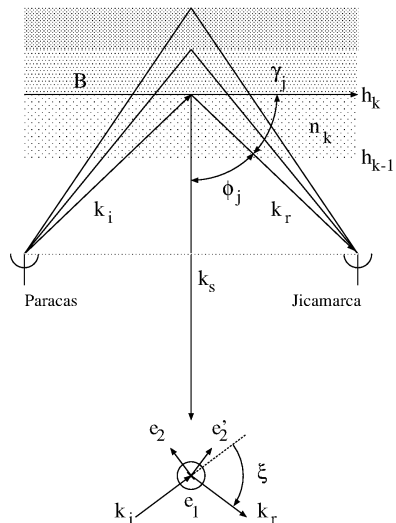
oblique obs. with Yagi array



oblique obs. AMISR-7



bistatic radar measurements

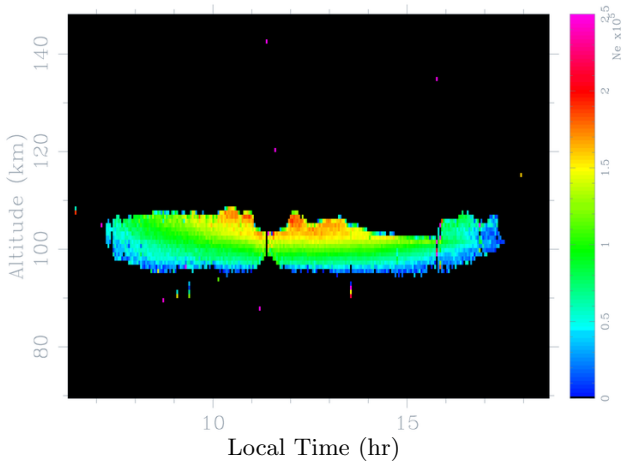


Paracas/ Jicamarca



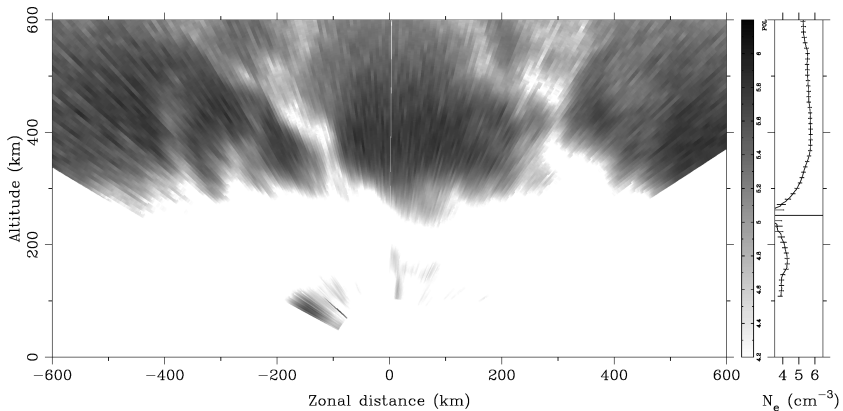
coherent scatter Faraday rotation

Fri Apr 23 18:39:52 2004

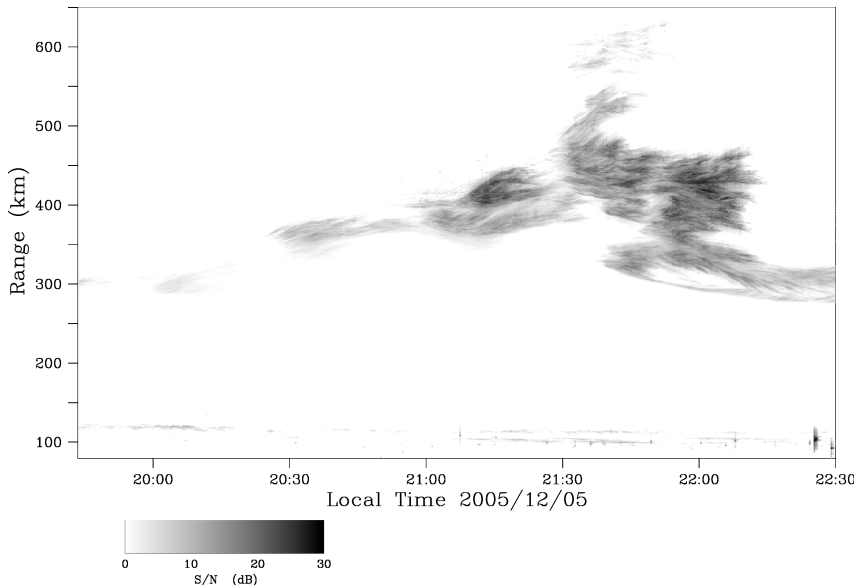


equatorial spread F

Wed Aug 11 10:09:04 2004

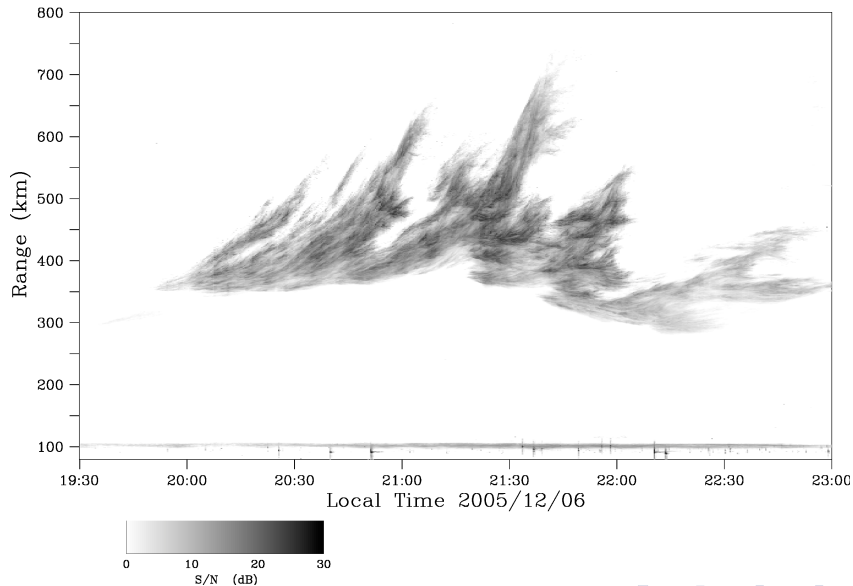


radar imagery

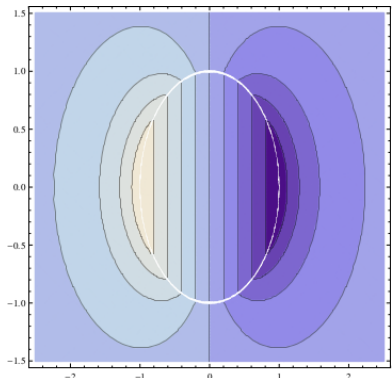


Dec 5

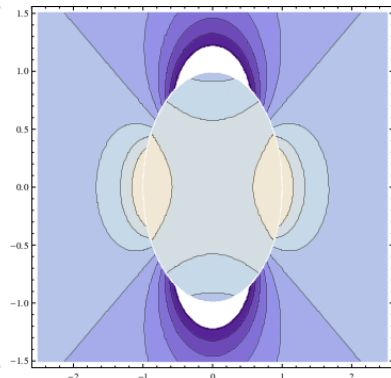
radar imagery



heuristic gRT theory: 3D warm plasmas; plan view



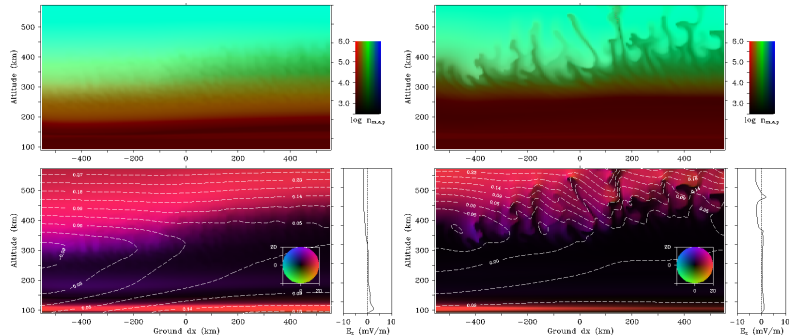
polarization



ambipolar diffusion

Drake, J. F., and J. D. Huba, *Phys. Rev. Lett.*, 58, 1987

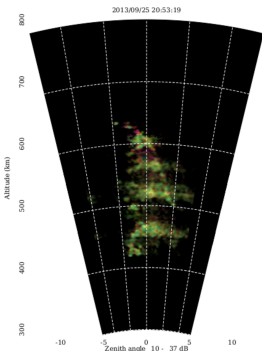
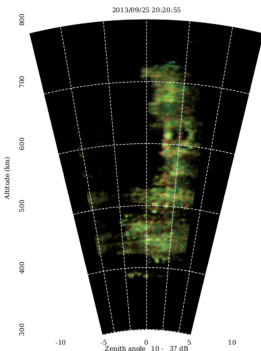
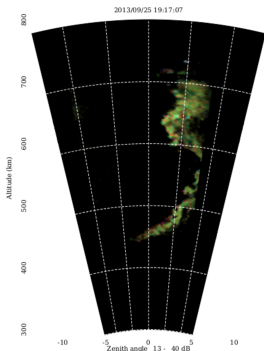
3D numerical simulation (less diamagnetic current)



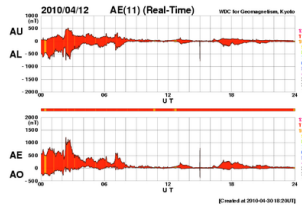
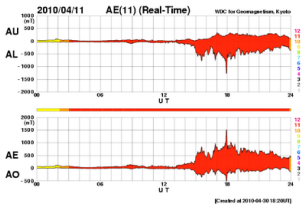
2345 UT + 25 min.

2345 UT + 75 min.

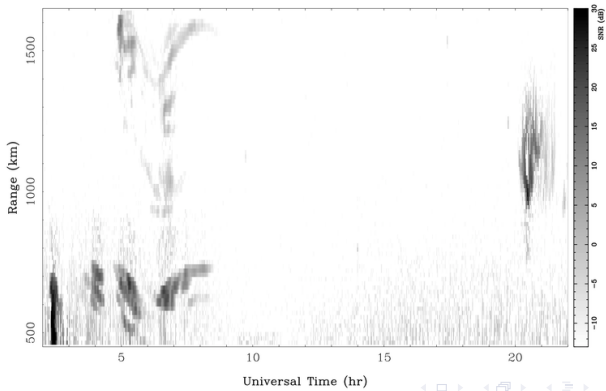
radar images – high activity



daytime spread F



ROJ Long Pulse: Mon Apr 12 15:30:52 2010



unique behavior of equatorial ionosphere

- Topside composition not quite consistent with diffusive equilibrium.
- Heat flows from photoelectrons to thermal electrons to ions to neutrals. Energetic electron transport especially important around dawn.
- Dynamics arise from wind-driven ionospheric currents, inhomogeneous, anisotropic conductivity, and the requirement of quasineutrality. Interesting flow features accompany regions with steep conductivity gradients.
- Most obvious features are the evening vortex in the *F* region and the equatorial electrojet in the *E* region.
- Plasma instabilities arise when the flow around conductivity irregularities is such as to deepen the irregularities. The main instabilities are FBGD in the *E* region and ESF in the *F* region.

topics for study

	sunrise	daytime	twilight	nighttime	ISR	CSR
mesospheric echoes		✓				✓
meteor echoes	✓					✓
electrojet	✓	✓	✓	✓		✓
valley echoes			✓			✓
150-km echoes		✓				✓
spread <i>F</i>				✓		✓
Faraday rotation	✓	✓	✓	✓	✓	
temperature overshoot	✓					✓
super rotation		✓		✓	✓	
evening vortex			✓			✓
topside		✓				✓